Pre-print submitted version

Tunable luminescent lead bromide complexes

Sang-Hyun Chin,[a] Jin Woo Choi,[b] Ziqi Hu,[a] Lorenzo Pietro Mardegan,[a] Michele Sessolo,[a] Henk J. Bolink*[a]

a. Instituto de Ciencia Molecular (ICMol), Universidad de Valencia, C/ Catedrático J. Beltrán 2, 46980 Paterna, Spain. E-mail: henk.bolink@uv.es
b. Advanced Functional Thin Films Department, Surface Technology Division, Korea Institute of Material Science (KIMS), 797 Changwondaero, Sungsan-Gu, Changwon 51508, Republic of Korea

Abstract

Lead halides are used extensively to prepare perovskite-based devices but less known that lead halides can also form luminescent complexes in solvents. Using polyethylene glycol solvent, lead bromide complex with photoluminescent quantum yield over 20 % is obtained and photoluminescent peak can be shifted around 50 nm with alkylammonium bromides.

Over the past decade, research towards organic-inorganic (hybrid) metal halide perovskite (MHP) photovoltaics has shown significant progress in power conversion efficiency (PCE), now exceeding 25 %.[1-7] Furthermore, the development of MHP light-emitting diodes has also advanced due to the high colour gamut, near-unity photoluminescence quantum yield (PLQY) and colour tunability within the entire visible region.[8-14] A particularly interesting class of perovskites are those in which larger organic cations are used to compensate the charge of the inorganic lead halide sheets. In these 2D perovskites, excitons are readily confined due to the high contrast between the dielectric constant of the organic moieties ($\varepsilon_{organic}$ ≈2.4) and inorganic octahedral counterpart ($\varepsilon_{inorganic}$ ≈6.1).[15-17] Yin et al. have described green luminescence from lead ions (Pb^{2+}) in zero-dimensional Cs_4PbBr_6 nanocrystals, with the recombination taking place within not yet identified green luminescent centres.[18] In this light it is interesting to note that main group

metal ions with an s^2 electronic configuration such as Pb^{2+} can also form simpler luminescent halide complexes ($PbBr_3^-$ and $PbBr_4^{2-}$) that stable in aprotic solvents (acetonitrile, dimethylformamide, dimethyl sulfoxide etc.).[19,20] The prospect of these coordination complexes in possible applications is discussed as well. As Dutta and Perkovic reported in 2002, lead bromide in acetonitrile (ACN) shows photoluminescence (PL) with a maximum at 610 nm, and a blue-shift upon addition of tetrabutylammonium bromide (TBABr).[19] Despite the inefficient luminescence (photoluminescent quantum yield (PLQY) ~0.5 %), this compound has been applied to sensing, and the photophysical property of lead halides in various solutions have been investigated.[20] However, there are only few reports on these materials and with very limited photoluminescent quantum yield (PLQY), so far with no comprehensive study about the luminescence mechanism.

Here we investigate the luminescent properties of lead bromide in electron donating polyethylene glycol (PEG) and study the effect of adding alkylammonium salts. The components used are similar to those used to prepare hybrid perovskites, yet the luminescent materials we study do not adopt that crystal structure. Nevertheless, we show that interesting luminescent properties are obtained for these complexes leading to new opportunities to obtain highly luminescent gels and solids. In addition, we propose a mechanism for the observed luminescence phenomena.

As mentioned in the introduction, the luminescence feature of lead bromide in acetonitrile has been reported. To investigate if a matrix with more electron donating character could improve the formation of the luminescent complex, we dissolved lead bromide in a low molecular weight (Mw) (liquid at room temperature) PEG at a concentration of 62.5mM. Fig. 1(a) shows the PL spectrum of this lead bromide solution. It shows an intense emission around 610 nm. The PL peak position is in accordance with the reported data for acetonitrile-based solutions, suggesting a similar origin of the luminescence. In the same fig. the excitation spectrum is also depicted which shows a rather sharp excitation peak around 330 nm. The PLQY of this solution is over 20 % (excitation 365 nm). This PLQY is much larger than what was previously reported for lead bromide in acetonitrile. This we tentatively attribute to the interaction between the PEG oxygen atoms and lead.[23,24] We also investigated the effect of the chain length of the PEGs used to dissolve the $PbBr_2$. The concentration is maintained (62.5mM) in all samples. These samples were characterized with steady state and time-resolved PL.

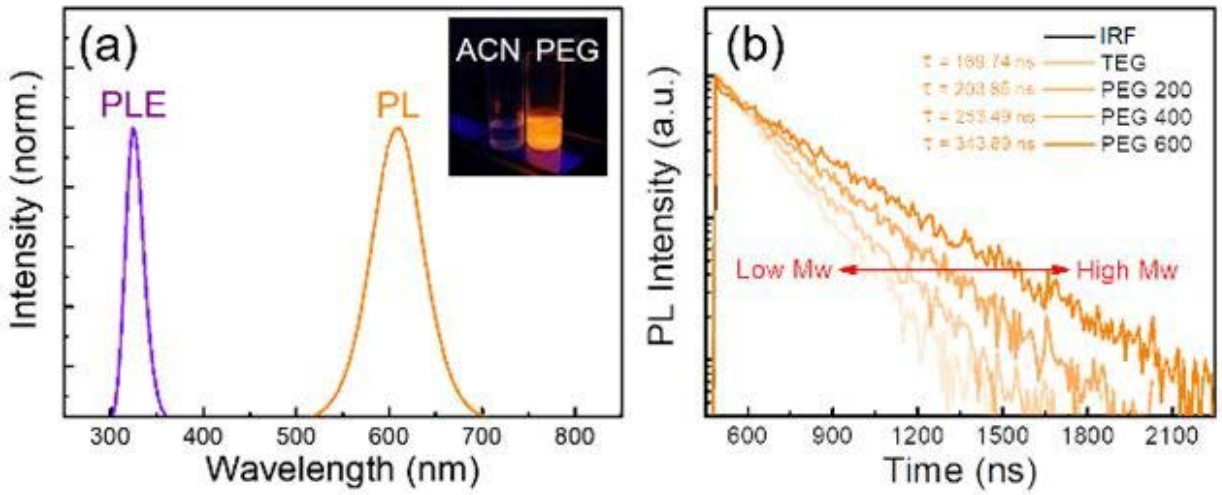

Fig. 1. (a) Photoluminescent and excitation spectra of lead bromide-PEG solution (inset: photographs of the lead bromide in ACN and PEG under, 365 nm excitation). (b) Chain-length dependant PL decay spectra of lead bromide-PEG solution.

The spectral position of the luminescence was found to be unvaried among the different materials, while we did observe an extended average decay lifetime for longer-chain PEGs in Fig. 1 (b) and Table 1. The PLQY was found to increase from 9% for the triethylene glycol (TEG), to 23 % for the PEG 600. The mechanism behind this behaviour is not yet clear, but the less efficient luminescence for low molecular weight (less viscous) PEGs might be related with a less constrained geometry and more pronounced vibrational quenching. In addition, halogenhydrogen interactions might assist the formation of Lewis acidbase adduct between oxygen and lead, as suggested by Yang Yang and co-workers.25 These findings imply that PEG polymers can be exploited as passivating hosts for lead halides, leading to simple and very luminescent materials.

In view of the recent developments of lead bromide containing perovskites we further investigated the optical properties of the most luminescent system, lead bromide and PEG 600, by adding monovalent cations that are also frequently used in the preparation of lead halide perovskites. In order to introduce these additional cations, a co-solvent (together with the PEG 600) was required. For this we selected dimethyl sulfoxide (DMSO). This solvent is particularly interesting as DMSO also interacts with lead bromide forming $PbBr_4^{2-}$, characterized by an excitation peak at 360 nm and a PL maximum at 560 nm (Fig. S1†).[26-28] Compared to the emission of $PbBr_2$ in PEG (610 nm) the emission of $PbBr_2$ in DMSO (560 nm) is blue shifted due to the transformation of the $PbBr_3^-$ (610 nm) into the $PbBr_4^{2-}$ (560 nm). The following salts were evaluated; methylammonium bromide (MABr), butylammonium bromide (BABr) and TBABr dissolved in DMSO (1.25M). The

ratio of RNH_3Br (alkylammonium Bromide) to $PbBr_2$ was kept constant at 2:1. The resulting PL spectra are depicted in Fig. 2. As expected, the emission peak for lead bromide DMSO is not affected when adding the different alkylammonium salts and remains around 560 nm (Fig. 2a).

Table 1. Photoluminescent characteristics of lead bromide in different polyethylene glycols.

	PL maximum (nm)	Average Decay time (ns)	PLQY (%)
TEG	610	170	9
PEG 200	610	204	12
PEG 400	610	253	17
PEG 600	610	344	23

However, when mixing lead bromide and the alkylammonium bromides in the presence of PEG the photoluminescence peak position is very different. Without adding the alkylammonium bromides the PL maximum is around 610 nm and upon addition of the alkylammonium bromides the PL maximum blue-shifts to 560 nm. (Fig. 2b). The largest shift in the PL spectra was observed, for the largest alkylammonium salt. With TBABr the PL maximum shifts to 560 nm which is similar to what is observed for pure $PbBr_2$ in DMSO. This indicates that there is a competition in the coordination of Pb^{2+} between PEG and DMSO, which is mediated by the alkylammonium bromide. A similar strong shift of the PL from 610 nm to 560 nm can be obtained for the same solution of lead bromide-MABr with DMSO-PEG co-solvent by using excess MABr (Supporting Information, Fig. S3†).

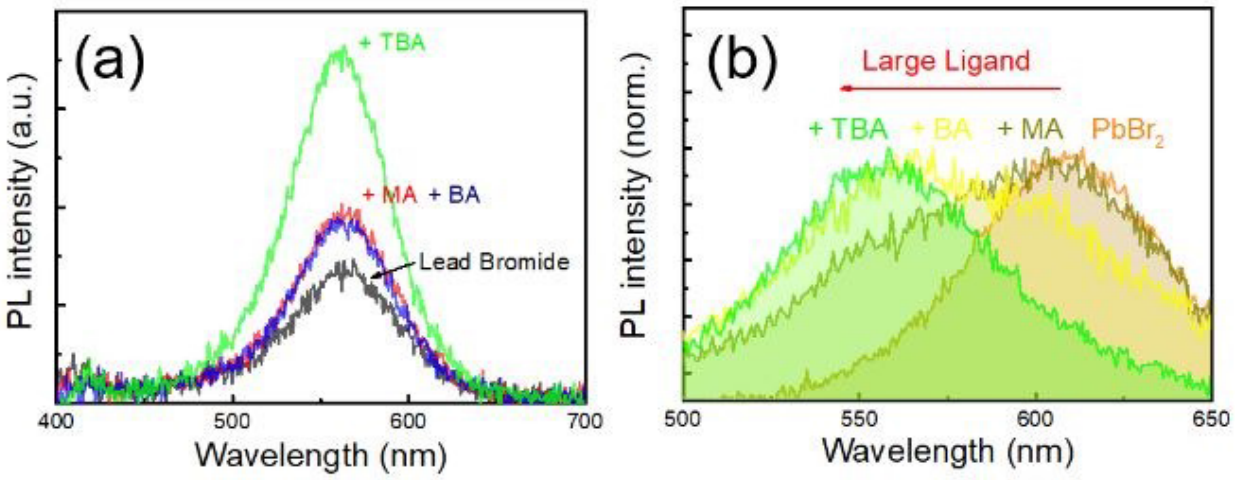

Fig. 2. (a) PL spectra of lead bromide and perovskite precursors in DMSO and (b) DMSO-PEG co-solvent

"The origin of the optical property of lead bromide in solution was initially investigated by Oldenburg and Vogler, who suggested a charge transfer model involving different lead bromides ($PbBr_3^-$ and $PbBr_4^{2-}$) to explain this phenomenon.27 In this model, charge transfer occurs from the bromide ions to lead (Fig. 3a). These transition mechanisms can be explained by metal-centred sp and ligand-tometal charge transfer (LMCT) transitions. Since an s^2 ion has an $^1S_0$ ground state and $^3P_0$, $^3P_1$, $^3P_2$ and $^1P_1$ excited states, the sp transition (ns to np) splits in several components. According to the report by Oldenburg and Vogler (reference 27), there can be 3 transitions described below:

A band: $^1S_0 \rightarrow {}^3P_1$ transition or $^1A_{1g} \rightarrow {}^3T_{1u}$ transition (in Oh symmetry)

B band: $^1S_0 \rightarrow {}^3P_2$ transition or $^1A_{1g} \rightarrow {}^3T_{1u}$ transition

C band: $^1S_0 \rightarrow {}^1P_1$ transition or $^1A_{1g} \rightarrow {}^1T_{1u}$ transition

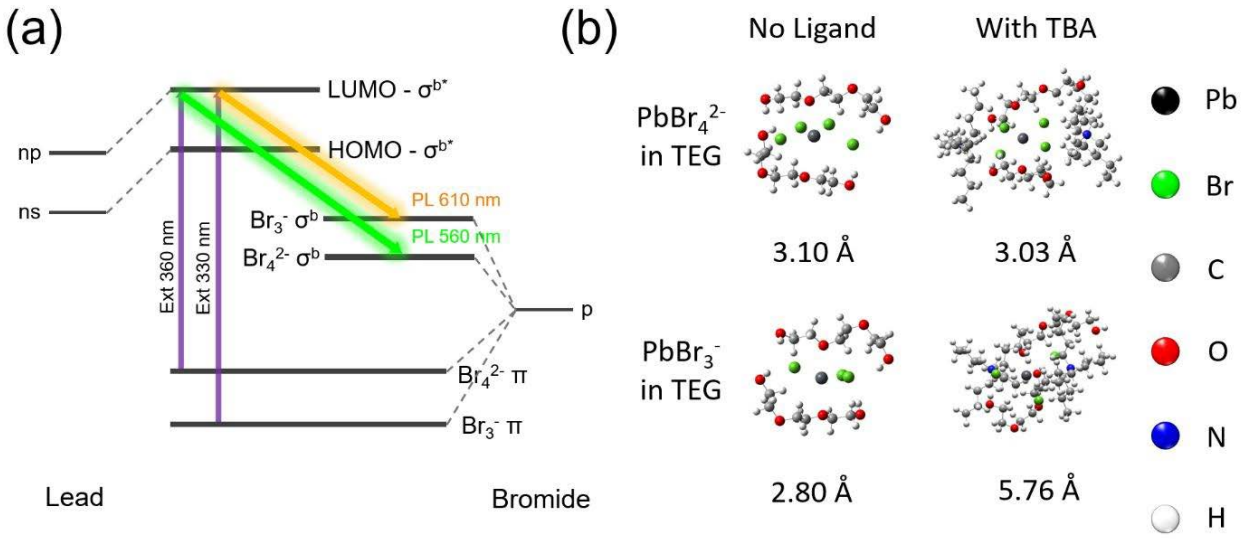

Fig. 3. (a) Schematic of the energy levels for the two different type of PbBr complexes ($PbBr_3^-$ to $PbBr_4^{2-}$) that according to Oldenburg and Vogler form. In it we depict the two emission wavelength observed and correlate it to the transition from the mixed σ* orbitals formed by charge transfer from the lead and bromide σ orbitals, to the groundstate σ obritals associated with Br_3^-, Br_4^{2-}. (b) Calculated position of the different atoms in the $PbBr_3^-$ and $PbBr_4^{2-}$ complexes in a prototype ethyleneoxide (TEG) with and without the presence of tetrabutylammonium. The results indicate a strong change in the lead-bromide distance for the two complexes affected by the presence of TBA, which is hence a possible mechanism for the observed shift in emission wavelengths.

In our complexes, $^1S_0 \rightarrow {}^3P_1$ transition and 1A1g→ 3T1u transition (in Oh symmetry) occur according to their study. In addition to these sp transitions, a LMCT transition can also occur which involves the promotion of a ligand electron from the filled p_π orbitals ($Br_3^-\pi$, $Br_4^{2-}\pi$) and p_σ orbitals ($Br_3^-\sigma$, $Br_4^{2-}\sigma$), to the empty antibonding p_σ orbitals of the metal. Eventually, these sp and LMCT transitions can mix. Depending on the number of the bromine ions in these complexes, the structures change due to different distortions. By adding alkylammonium, we could turn $PbBr_3^-$ into $PbBr_4^{2-}$. These two complexes have trigonal pyramidal (C_{3v}) and disphenoidal (C_{2v}) structure, respectively, which leads to different energy levels and excitations. In an attempt to verify our hypothesis: that the property change is related to the difference in the solvent coordination, by "alkylammonium bromide introduction" which induces the $PbBr_3^-$ to $PbBr_4^{2-}$ transformation, we performed theoretical calculations. Using Gaussian09 as the simulation software…." Using Gaussian09 as the simulation software we calculated the geometrical orientation and distance between solvents, ligands, lead and bromide. In order to simplify the model, the small TEG molecule was selected as the PEG type additive to the lead bromide-ligand system. The calculated distances between Pb and O are presented in Fig. 3b.[29] The initial Pb-O distances in the complexes $PbBr_4^{2-}$ and $PbBr_3^-$ are 3.10 Å and 2.80 Å, respectively. After introducing the large

TBABr salt, the Pb-O distance decreases to 3.03 Å for $PbBr_4^{2-}$ and increases to 5.76 Å in the case of $PbBr_3^-$. (Fig. S4a†). In addition, the $PbBr_3^-$-TEG complex is unstable as the Br anions dissociate. This does not happen with $PbBr_4^{2-}$ which remains intact. This implies that the $PbBr_3^-$ is the less favoured structure and transforms into $PbBr_4^{2-}$ in TEG in the presence of TBABr. This is in line with the trend observed in the PL spectra, i.e. adding TBABr results in an effective blue-shift eventually coinciding with the PL of $PbBr_4^{2-}$ in pure DMSO. The introduction of TBABr leads to a large increase in the Pb-O distance and hence the DMSO to Pb^{2+} interaction becomes the dominant one. This leads to an increase of the green emission from the $PbBr_4^{2-}$ species. The stronger interaction between DMSO and Pb^{2+} also explains the dramatic decrease of PLQY after injecting DMSO in lead bromide-PEG solutions, from 23% to only 2% (Table S1†). The observed photoluminescence spectra are stable in ambient conditions without any noticeable decrease for one week (Fig. S5†).

The simulations also confirm that there is an interaction between hydrogen and halide atoms. We have used quantum theory of atom in molecule (QTAIM) to estimate this interaction.[30,31]

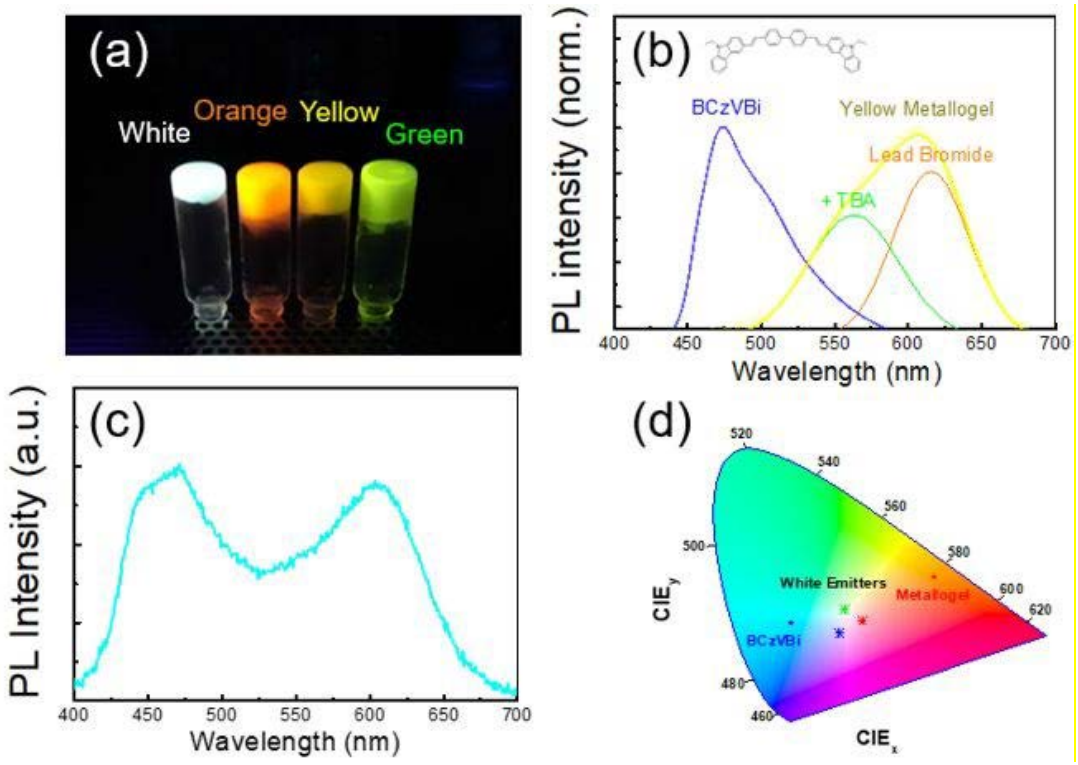

Fig. 4. (a) Luminescent complexes under UV. (b) PL spectra of blue-emitting BCzVBi dye and yellow-emissive solution. (c) PL spectrum and (d) CIEcoordinates of White and yellow-emissive solution and BCzVBi.

The calculated figures showing the different interactions between the ions and elements are shown in Fig. S4b†. As mentioned before, such a halide hydrogen interaction may assist the formation of Lewis acid-base adduct between oxygen and lead, according to Yang Yang and co-workers.[25]

The use of chloride salts ($PbCl_2$ and TBACl) results in a blueshifted PL as compared to the bromide mixture (from 560 nm to 510 nm), similarly to what is observed in perovskite semiconductors (Fig. S6†).[17,32] Interestingly, the lead chloride complex with TBA is more luminescent (PLQYs of 7%, while only 3% for bromides).

The results presented so far indicate that lead halide-PEG mixtures have improved luminescent properties compared to other lead halides solutions previously reported. As a proof-of concept application of these materials, we prepared several luminescent metallogel-like solutions with different emission colours.[32,33] By employing PEG 600, with a melting point of about 15 ºC, luminescent gels with orange ($PbBr_2$:PEG), green ($PbBr_2$:TBABr:PEG) and yellow (mixture of the orange and green gels) emissions are readily obtained by decreasing the temperature to below 15 ºC (Fig. 4a). White fluorescent gels are obtained by adding the dye 4,4'-Bis(9-ethyl-3-carbazovinylene)-1,1'-biphenyl (BCzVBi) to PEG. Fig. 4b shows the PL spectra of the as-prepared materials, covering the whole visible region of the spectrum. Hence, by mixing the BCzVBi with the yellow emissive metallogel (YG) which consist of lead bromide+TBABr in PEG, white light-emitting metallogels can also be prepared (spectrum in Fig. 4c). Fig. 4d shows the corresponding CIE colour coordinates (Commission internationale de l'éclairage 1931). In this figure we also depict the colour coordinates of additional white materials obtained with different mixtures of the precursor gels (details in Fig. S7† and Table S2†). Besides this proof-of-concept, there is room for improvement both regarding the simple polymer used (PEG), and by replacing lead with less toxic metal centres.34-36 Decreasing the temperature to 0 □C, does not change the appearance nor the emission colour as depicted in Fig. S8 in the ESI.

Conclusions

In conclusion, dissolving lead halide salts in electron donating solvents leads to efficient luminescent solution and gels. The addition of stronger electron donors leads to a strong shift in the luminescent wavelength, clearly detectable by the human eye. As the compounds used to prepare the luminescent solutions are also used to prepare lead halide perovskites, it is possible that similar emitting centres are co-formed in the formation of perovskite films from coordinating

solvents. A mechanism for the different emission wavelengths is proposed based on the different coordination of the Pb^{2+} ions. Evidence for this was obtained from a theoretical simulation mapping the Pb-O interaction length. The here presented room temperature luminescent gels are of interest for applications in phosphors, bio-imaging and environmental sensing.

Conflicts of interest

There are no conflicts to declare.

Acknowledgement

This work has received funding from the Spanish Ministry of Science, Innovation and Universities (ex-MINECO) via the Unidad de Excelencia María de Maeztu CEX2019-000919-M and MAT2017-88821-R, PCI2019-111829-2 and the Comunitat Valenciana IDIFEDER/2018/061. M.S. acknowledges the MINECO for his RyC.

References

1 A. Kojima, K. Teshima, Y. Shirai and T. Miyasaka, J. Am. Chem. Soc., 2009, 131, 6050-6051.

2 H.-S. Kim, C.-R. Lee, J.-H. Im, K.-B. Lee, T. Moehl, A. Marchioro, S.-J. Moon, R. Humphry-Baker, J.-H. Yum, J. E. Moser, M. Grätzel and N.-G. Park, Sci. Rep., 2012, 2, 591.

3 M. M. Lee, J. Teuscher, T. Miyasaka, T. N. Murakami and H. J. Snaith, Science, 2012, 338, 643–647.

4 O. Malinkiewicz, A. Yella, Y. H. Lee, G. M. Espallargas, M. Graetzel, M. K. Nazeeruddin and Bolink, H. J., Nat. Photon., 2014, 8, 128-132.

5 M. D. Xiao, F. Huang, W. Huang, Y. Dkhissi, Y. Zhu, J. Etheridge, A. Gray-Weale, U. Bach, Y.-B. Cheng and L. A. Spiccia, Angew. Chem., Int. Ed., 2014, 53, 9898-9903.

6 W. S. Yang, B.-W. Park, E. H. Jang, N. J. Jeon, Y. C. Kim, D. U. Lee, S. S. Shin, J. Seo, E. K. Kim, J. H. Noh and S. I. Seok, Science, 2017, 356, 1376-1379.

7 NREL, https://www.nrel.gov/pv/cell-efficiency.html, July, 2020.

8 Z.-K. Tan, R. S. Moghaddam, M. L. Lai, P. Docampo, R. Higler, F. Deschler, M. Price, A. Sadhanala, L. M. Pazos, D. Credgington, R. Hanusch, T. Bein, H. J. Snaith and R. H. Friend, Nat. Nanotechnol., 2014, 9, 687-692.

9 H. Cho, S.-H. Jeong, M.-H. Park, Y.-H. Kim, C. Wolf, C.-L. Lee, J. H. Heo, A. Sadhanala, N. Myoung, S. Yoo, S. H. Im, R. H. Friend and T.-W. Lee, Science, 2015, 350, 1222-1225.

10 M.-G. La-Placa, G. Longo, A. Babaei, L. Martinez-Sarti, M. Sessolo and H. J. Bolink, Chem. Commun., 2017, 53, 8707-8710.

11 J.-W. Lee, Y. J. Choi, J.-M. Yang, S. Ham, S. K. Jeon, J. Y. Lee, Y.-H. Song, E. K. Ji, D.-H. Yoon, S. Seo, H. Shin, G. S. Han, H. S. Jung, D. Kim and N.-G. Park, ACS Nano, 2017, 11, 3311–3319.

12 K. Lin, J. Xing, L. N. Quan, F. P. G. de Arquer, X. Gong, J. Lu, L. Xie, W. Zhao, D. Zhang, C. Yan, W. Li, X. Liu, Y. Lu, J. Kirman, E. H. Sargent, Q. Xiong and Z. Wei, Nature, 2018, 562, 245–248.

13 S.-H. Chin, J. W. Choi, H. Woo, J. H. Kim, H. S. Lee and C.-L. Lee, Nanoscale, 2019, 11, 5861-5867.

14 H. C. Woo, J. W. Choi, J. Shin, S.-H. Chin, M. H. Ann and C.-L. Lee, J. Phys. Chem. Lett., 2018, 9, 4066–4074.

15 M. Era, S. Morimoto, T. Tsutsui and S. Saito, Appl. Phys. Lett., 1994, 65, 676.

16 T. Hattori, T. Taira, M. Era, T. Tsutsui, S. Saito, Chem. Phys. Lett., 1996, 254, 103-108.

17 Y.-H. Kim, H. Cho, J. H. Heo, T.-S. Kim, N. S. Myoung, C.-L. Lee, S. H. Im and T.-W. Lee, Adv. Mater., 2015, 27, 1248-1254.

18 J. Yin, Y. Zhang, A. Bruno, C. Soci, O. M. Bakr, J.-L. Brédas and O. F. Mohammed, ACS Energy Lett., 2017, 2, 2805-2811.

19 S. K. Dutta and M. K. Perkovic, Inorg. Chem., 2002, 41, 6938-6940.

20 S.-H. Li, F.-R. Chen, Y.-F. Zhou and J.-G. Xu, Analyst, 2009, 134, 443-446.

21 J. Franck and E. Rabinowitsch, Trans. Faraday Soc, 1934, 30, 120-130.

22 J. S. Mayell and A. J. Bard, J. Am. Chem. Soc., 1963, 85, 421-425.

23 S. G. R. Bade, J. Li, X. Shan, Y. Ling, Y. Tian, T. Dilbeck, T. Besara, T. Geske, H. Gao, B. Ma, K. Hanson, T. Siegrist, C. Xu and Z. Yu, ACS Nano, 2016, 10, 1795-1801.

24 L., Song, X. Guo, Y. Hu, Y., Lv, J. Lin, Z. Liu, Y. Fan and X. Liu, J. Phys. Chem. Lett. 2017, 8, 4148-4154.

25 R. Wang, J. Xue, K.-L. Wang, Z.-K. Wang, Y. Luo, D. Fenning, G. Xu, S. Nuryyeva, T. Huang, Y. Zhao, J. L. Yang, J. Zhu, M. Wang, S. Tan, I. Yavuz, K. N. Houk and Y. Yang, Science, 2019, 366, 1509-1513.

26 K. Oldenburg and A. Volger, Zeitschrift für Naturforschung B 1993, 48, 1519–1523.

27 S. J. Yoon, K. G. Stamplecoskie, P. V. Kamat, J. Phys. Chem. Lett. 2016, 7, 1368−1373.

28 A. Ray, D. Maggioni, D. Baranov, Z. Dang, M. Prato, Q. A. Akkerman, L. Goldoni, E. Caneva, L. Manna and A. L. Abdelhady, Chem. Mater. 2019, 31, 7761−7769.

29 M. J. Frisch, G. W. Trucks, H. B. Schlegel, G. E. Scuseria, M. A. Robb, J. R. Cheeseman, G. Scalmani, V. Barone, G. A. Petersson, H. Nakatsuji, X. Li, M. Caricato, A. Marenich, J. Bloino, B. G. Janesko, R. Gomperts, B. Mennucci, H. P. Hratchian, J. V. Ortiz, A. F. Izmaylov, J. L. Sonnenberg, D. Williams-Young, F. Ding, F. Lipparini, F. Egidi, J. Goings, B. Peng, A. Petrone, T. Henderson, D. Ranasinghe, V. G. Zakrzewski, J. Gao, N. Rega, G. Zheng, W. Liang, M. Hada, M. Ehara, K. Toyota, R. Fukuda, J. Hasegawa, M. Ishida, T. Nakajima, Y. Honda, O. Kitao, H. Nakai, T. Vreven, K. Throssell, J. A. Montgomery, Jr., J. E. Peralta, F. Ogliaro, M. Bearpark, J. J. Heyd, E. Brothers, K. N. Kudin, V. N. Staroverov, T. Keith, R. Kobayashi, J. Normand, K. Raghavachari, A. Rendell, J. C. Burant, S. S. Iyengar, J. Tomasi, M. Cossi, J. M. Millam, M. Klene, C. Adamo, R. Cammi, J. W. Ochterski, R. L. Martin, K. Morokuma, O. Farkas, J. B. Foresman, and D. J. Fox, Gaussian 09, Revision A.02, Gaussian, Inc., Wallingford CT, 2016.

30 R. F. Bader, Acc. Chem. Res. 1985, 18, 9-15.

31 T. Lu, F. W. Chen, J. Comput. Chem. 2012, 33, 580-592.

32 H. Wu, J. Zheng, A.-L. Kjøniksen, W. Wang, Y. Zhang and J. Ma, Adv. Mater. 2019, 31, 1806204.

33 S. Mollick, T. N. Mandal, A. Jana, S. Fajala and S. K. Ghosh, Chem. Sci., 2019, 10, 10524-10530.

34 L.-J. Xu, C.-Z. Sun, H. Xiao, Y. Wu and Z.-N. Chen, Adv. Mater., 2017, 29, 1605739.

35 P. Sebastia-Luna, J. Navarro-Alapont, M. Sessolo, F. Palazon, and H. J. Bolink, Chem. Mater., 2019, 31, 10205-10210.

36 Y. El Ajjouri, V. S. Chirvony, N. Vassilyeva, M. Sessolo, F. Palazon and H. J. Bolink, J. Mater. Chem. C, 2019, 7, 6236-6240.

Electronic Supplementary Information

Tunable luminescent lead bromide complexes

Sang-Hyun Chin,[a] Jin Woo Choi,[b] Ziqi Hu,[a] Lorenzo Pietro Mardegan,[a] Michele Sessolo,[a] Henk J. Bolink*[a]

a. Instituto de Ciencia Molecular (ICMol), Universidad de Valencia, C/Catedratico J. Beltran 2, 46980 Paterna (Valencia), Spain. E-mail: henk.bolink@uv.es

b. Advanced Functional Thin Films Department, Surface Technology Division, Korea Institute of Material Science (KIMS), 797 Changwondaero, Sungsan-Gu, Changwon, Gyeongnam 51508, Republic of Korea.

I. Materials and Methods

i. Preparation of the lead halides in poly(ethylene glycol) Lead bromide, lead chloride, tetrabutylammonium bromide (TBABr), tetrabutylammonium chloride (TBACl), dimethylsulfoxide (DMSO), Poly(ethylene glycol) (PEG) 200 and 400 are purchased from Sigma-Aldrich. Tri-ethylene glycol and PEG 600 are purchased from Alfa Aesar. Butylammonium bromide is from Dyesol and methylammonium bromide is from Lumtec. Every solute, alkylammonium halide or lead halide, is dissolved and stirred overnight in DMSO-PEG co-solvent (1:10 volume ratio) except lead bromide in PEG (In Figure 1). For perfect solvation, lead halide solution is diluted until 62.5 mM (1/16 M). All procedures are processed in air

ii. Preparation of white-emissive metallogel 4,4'-Bis(9-ethyl-3-carbazovinylene)-1,1'-biphenyl (BCzVBi) is purchased from Lumtec. This blue-emissive organic dye is dispersed in tetrabutylammonium lead bromide based yellow-emissive metallogel with DMSO-PEG 600 co-solvent. These yellow-emissive agents, yellow metallogels (YGs) are obtained by stoichiometric control of TBABr and lead bromide. (TBABr : lead bromide = 0.5:1 in YG 1, 1:1 in YG 2) with consistent concentration of lead bromide, 62.5 mM. For the phase-transition to gel, temperature is decreased under 15℃. All procedures are processed in air

II. Characterization

i. Photoluminescent excitation and emission spectra measurement The PL spectra were collected using a Xe lamp coupled to a monochromator as the excitation source and a spectrometer (Hamamatsu C9920-02 with a Hamamatsu PMA-11 optical detector). The wavelength of excitation sources were 365 nm and 340 nm for bromides and chlorides. PLQY values were obtained using a Xe lamp coupled to a monochromator as the excitation source and an integrating sphere coupled to a same spectrometer. The instrumental error is ≈1%. The PL excitation spectra were collected by Edinburgh FLS1000 using a µF2 Xe lamp and single-photon counting vis-PMT 980.

ii. Photoluminescence decay time measurement PL decays were measured using a compact fluorescence lifetime spectrometer C11367, Quantaurus Tau. The excitation sources were, consistently 365 nm and 340 nm LEDs for bromide and chloride, respectively. PL lifetime measurement software U11487 was used to register the data. the PL decays were fitted with a biexponential function.

III. Simulation

Density Functional Theory-calculation All the calculations are carried out using Gaussian09 program at the level of m06-2x/def2-tzvp for all atoms and SDD pseudopotential for Pb atoms with dispersion correction GD3 method. The optimized structures are further examined by frequency analysis to confirm that true local minima are achieved. In addition, quantum theory of atom in molecule (QTAIM) is applied to visualize bonds.

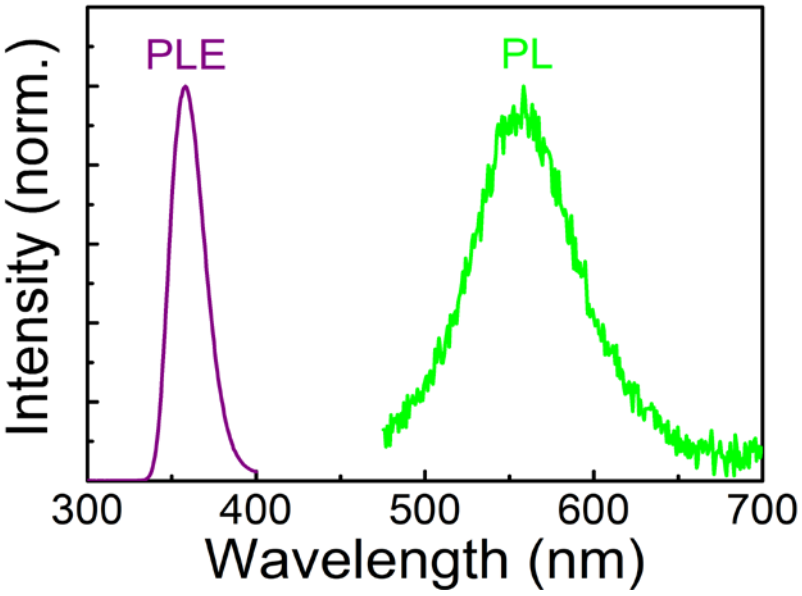

Fig. S1. Photoluminescent and excitation spectra of DMSO

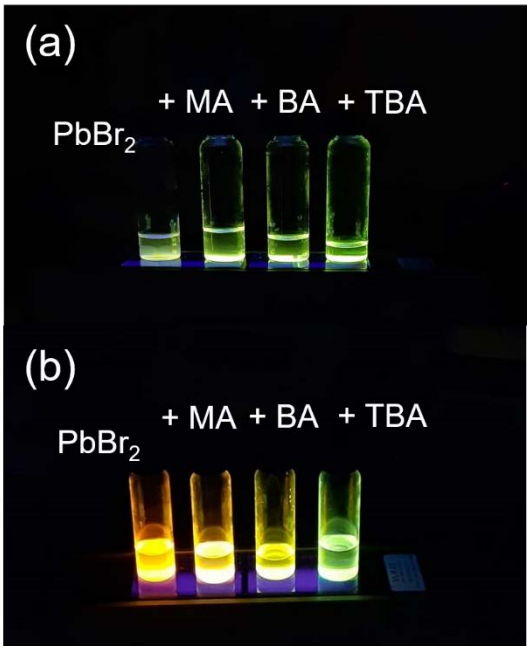

Fig. S2. (a) Luminescent lead bromide and perovskite precursor solutions in DMSO and (b) DMSO-PEG co-solvent on UV lamp

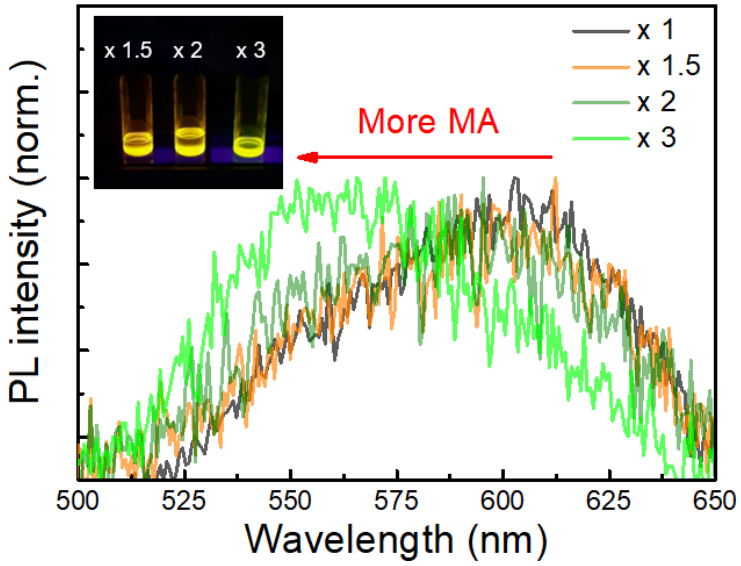

Fig. S3. Excess MABr concentration-dependant photoluminescent spectra

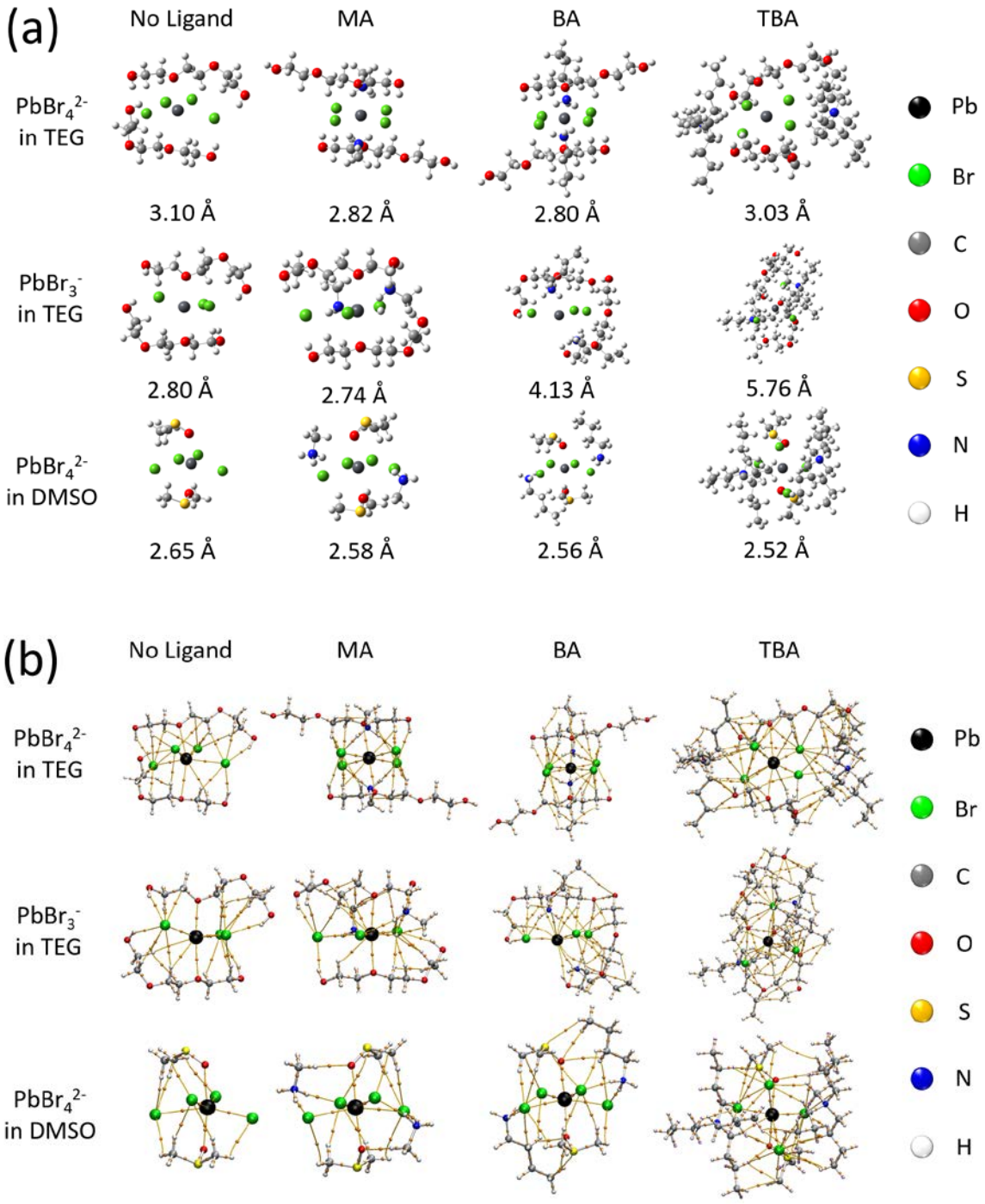

Fig. S4. (a) Theoretical calculation of Pb-O distances in lead bromide-solvent system with and without various ligands. (b) Visualized interaction via Quantum theory of atom in molecule (QTAIM).

Note: The covalent bonds are visualized as white lines while the chemical interactions are yellow. The calculations show that $PbBr_3^-$ in TEG is not stable in the presence of large ligands. The Br anion dissociates in those systems.

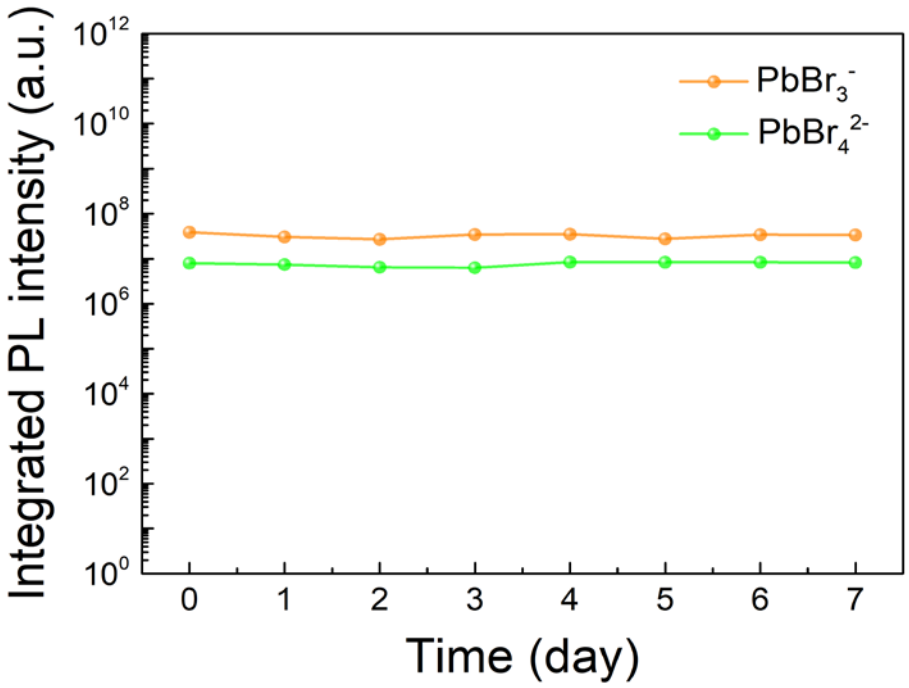

Fig. S5. PL stability of $PbBr_3^-$ and $PbBr_4^{2-}$ complexes

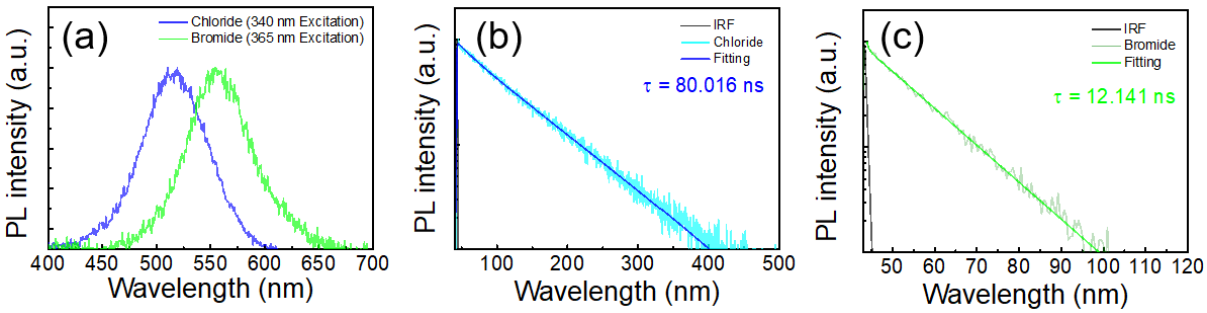

Fig. S6. (a) Photoluminescent spectra of lead chloride + TBACl and lead bromide + TBABr (TBAX is 2-fold to lead halide). Decay curves of (b) chloride and (c) bromide.

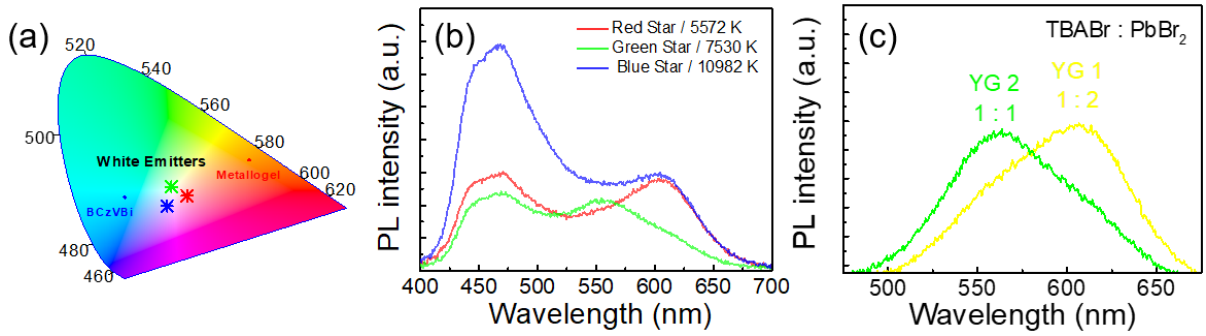

Figure S7. (a) Emissive character of BCzVBi, yellow metallogel and white metallogel set on CIE coordinate. PL spectra of (b) white-emissive metallogel set and (c) yellow-emissive metallogel set.

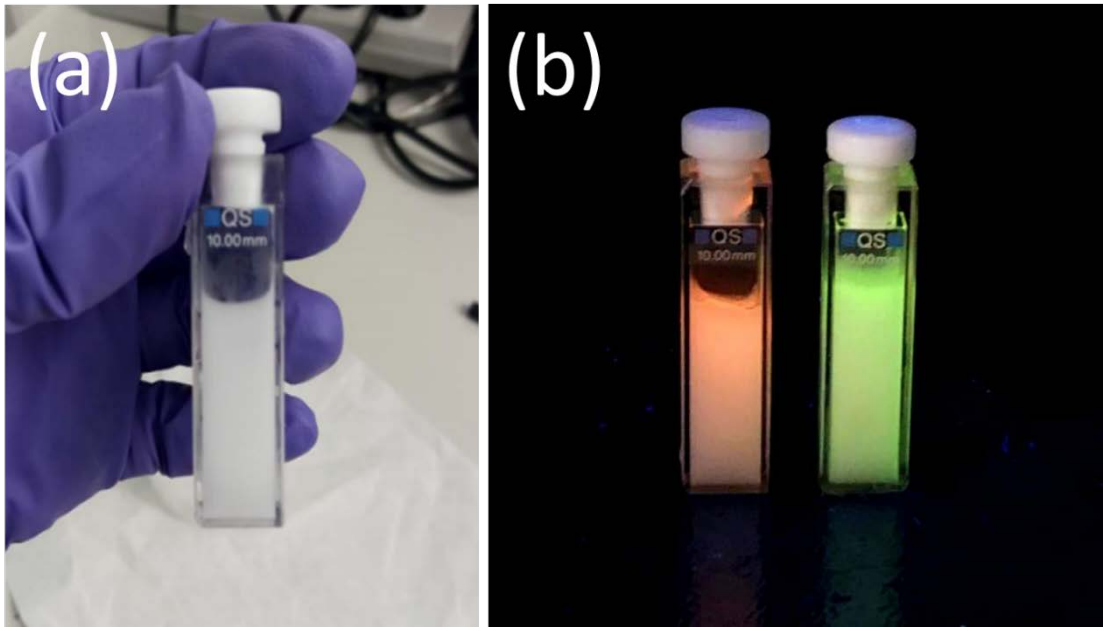

Figure S8. Gel phase sample at 0 °C for optical characterizations. (a) under white light illumination and (b) under UV illumination for a sample without (orange fluorescence) and with alkylammonium bromide (green fluorescence).

Table S1. PLQY Table

Solute	Solvent	PLQY (%)	Note
$PbBr_2$	DMF	1.6	
$PbBr_2$	DMSO	0.7	
$PbBr_2$ + 2MABr	DMSO	1.1	
$PbBr_2$ + 2BABr	DMSO	1.0	
$PbBr_2$ + 2TBABr	DMSO	2.1	
$PbBr_2$	TEG	9.3	
$PbBr_2$	PEG 200	12.3	
$PbBr_2$	PEG 400	16.6	
$PbBr_2$	PEG 600	23.4	- Due to the phase transition of PEG 600 on 15℃, measurements are conducted over 20℃. - The volume ratio between DMSO and PEG 600 in co-solvent is 1:10. - DMSO decreases PLQY of PEG-based solution (refer to $PbBr_2$ in DMSO and DMSO + PEG 600). - Pure $PbCl_2$ is unable to be dissolved in PEG. - The PLQY of white-emissive metallogel (W1-3) is highly dependent on the concentration of BCzVBi dye.
$PbBr_2$	DMSO + PEG 600	2.1	
$PbBr_2$ + 1.5MABr	DMSO + PEG 600	2.7	
$PbBr_2$ + 2MABr	DMSO + PEG 600	2.5	
$PbBr_2$ + 3MABr	DMSO + PEG 600	2.0	
$PbBr_2$ + 2BABr	DMSO + PEG 600	2.2	
$PbBr_2$ + 2TBABr	DMSO + PEG 600	2.7	
$PbCl_2$ + 2TBACl	DMSO + PEG 600	7.4	
YG1 set	DMSO + PEG 600	4.0	
YG2 set	DMSO + PEG 600	3.7	
W1 set	DMSO + PEG 600	7.4	
W2 set	DMSO + PEG 600	5.4	
W3 set	DMSO + PEG 600	9.2	

Table S2. Color of White emitters

	Concentration of BCzVBi	CIE coordinate (CIE_x, CIE_y)	Color temperature (T_c)
W1 (Red Star)	0.125 g/l in YG 1	0.331, 0.311	5572 K
W2 (Green Star)	0.625 g/l in YG 2	0.291, 0.345	7530 K
W3 (Blue Star)	1.250 g/l in YG 1	0.280, 0.273	10982 K

Color temperature (T_c) set is calculated by McCamy's approximation which is shown below.

$$n = \frac{(CIE_x - 0.3320)}{(0.1858 - CIE_y)}$$

$$T_c\,(\mathrm{K}) = 437\,n^3 + 3601\,n^2 + 6861\,n + 5517$$